

Gear fatigue of austempered ductile iron (ADI): an overview of numerical studies at UTFPR

Roberto Luís de Assumpção ^{1*} 

Marco Antônio Luersen ² 

Carlos Henrique da Silva ¹ 

Abstract

ADIs are very versatile materials and can provide high performance in situations involving fatigue and wear. To understand the effect of graphite nodules on fatigue strength of ADIs, an interesting way of studying are the numerical analyzes through the Finite Element Method (FEM). UTFPR in partnership with TUPY S.A., especially under the supervision of Prof. Dr. Wilson L. Guesser, has carried out several studies via FEM in order to generate enough interesting knowledge, both for the foundry company and for the end user of ADI. From the results of these studies, it was found that, in general, although smaller graphite nodules have a slight tendency to nucleate cracks more quickly, their characteristics of relieving stresses and generating a branched mesh of interconnected cracks, which absorb energy at the crack tips, makes ADI with small nodules becomes a very competitive material in gear manufacturing.

Keywords: Austempered ductil iron (ADI); Finite element method (FEM); Fatigue; Gear.

1 Introduction

Austempered Ductile Irons (ADIs) are very versatile materials and can provide adequate performance in situations involving abrasive wear. Typical examples of applications are parts of earthmoving and mining equipment. In the automotive industry, the use of ADIs is mainly focused on components subjected to high mechanical stresses associated with of impact loads, as an example the parts of vehicle suspension [1,2]. In this case, materials grades 1 and 2 are selected according to ASTM-06 A897M, which combine good mechanical strength with toughness [3].

ADI as gear material has been the subject of several studies [4-9], aiming to reduce manufacturing and machining costs and noise in service, in addition to improved gearing efficiency. ADI has been see as a possible substitute for steel alloy at different loading levels, as it combines adequate mechanical strength and high ductility, highlighting resistance to fatigue and wear [10].

Guesser et al. [11] present an interesting alternative for the production of gears from nodular cast iron bars obtained by continuous casting to replace traditionally cemented and tempered alloy steel. ADIs can be quite competitive in medium severity applications.

According to [12] and [13], ADI may present resistance to contact fatigue comparable to that of AISI 4140 steel [11], with a reduction of about 10% in weight of the components and be a financially advantageous option, as it requires heat

treatment at lower temperatures that those used for other steels, thus reducing the demand of electricity.

The contact fatigue phenomenon is the main responsible for most damages on gear faces, thus, nucleation and crack propagation phases (surface and subsurface) are directly related to the total number of life cycles of these components.

In gears manufactured in ADI, graphite nodules, despite promoting greater ductility to the material, also act as stress concentrators, which make them very important in the crack nucleation phase, as well as the characteristics of size, shape and distribution of the nodules are more relevant in the propagation stage of these cracks.

To understand the influence of nodules on contact fatigue life, an interesting way is to use computational tools, with the usage of numerical analysis through Finite Element Method (FEM). Using the traditional solid mechanics approach, it is possible to propose stress concentration factors and thus quantitatively understand the effects of size and distribution of nodules in the ADI matrix. Applying the principles of linear elastic fracture mechanics (LEFM) it is possible to observe more clearly, how the nucleation and crack propagation phases are correlated with the experimental results performed with ADI gears.

In partnership with Tupy S.A. company, represented by Prof. Dr. Wilson Luiz Guesser, several researches have been developed at UTFPR (Surface and Contact Laboratory - LASC and Structural Mechanics Laboratory - LAMES).

¹Laboratório de Superfícies e Contato, LASC, Universidade Tecnológica Federal do Paraná, UTFPR, Curitiba, PR, Brasil.

²Laboratório de Mecânica Estrutural, LAMES, Universidade Tecnológica Federal do Paraná, UTFPR, Curitiba, PR, Brasil.

*Corresponding author: robertolassumpcao@gmail.com



Always in search of a better understanding of the influence of the characteristics of graphite nodules (size, quantity and distribution) of the ADI obtained by continuous casting, in its fatigue life. Figure 1 shows the results of FZG wear tests on several alloy steels and two types of ADI. This better performance of failure probability between the calls, ADI1 and ADI2, is one of the main focus of interest of the FEM numerical analysis presented in this work.

2 Numerical procedures

The FEM works developed within the TUPY-UTFPR partnership were based on the results of Figure 1 [11]. Thus, the characteristics of the tests and ADI tested are presented in the tables below as follows:

Composition and thermochemical treatments of ADI – Table 1;

Geometric characteristics of gears tested in FZG test rig – Table 2;

Mechanical characteristics and properties of ADI – Table 3;

2.1 Flowchart studies

The stages of development of the numerical analyzes performed at UTFPR with FEM approaches can be seen in the flowchart shown in Figure 2.

2.2 FEM analyzes and corresponding goals

Table 4 summarizes the most relevant works of the TUPY-UTFPR partnership, presenting some characteristics of the numerical analyzes and the main objectives of each research.

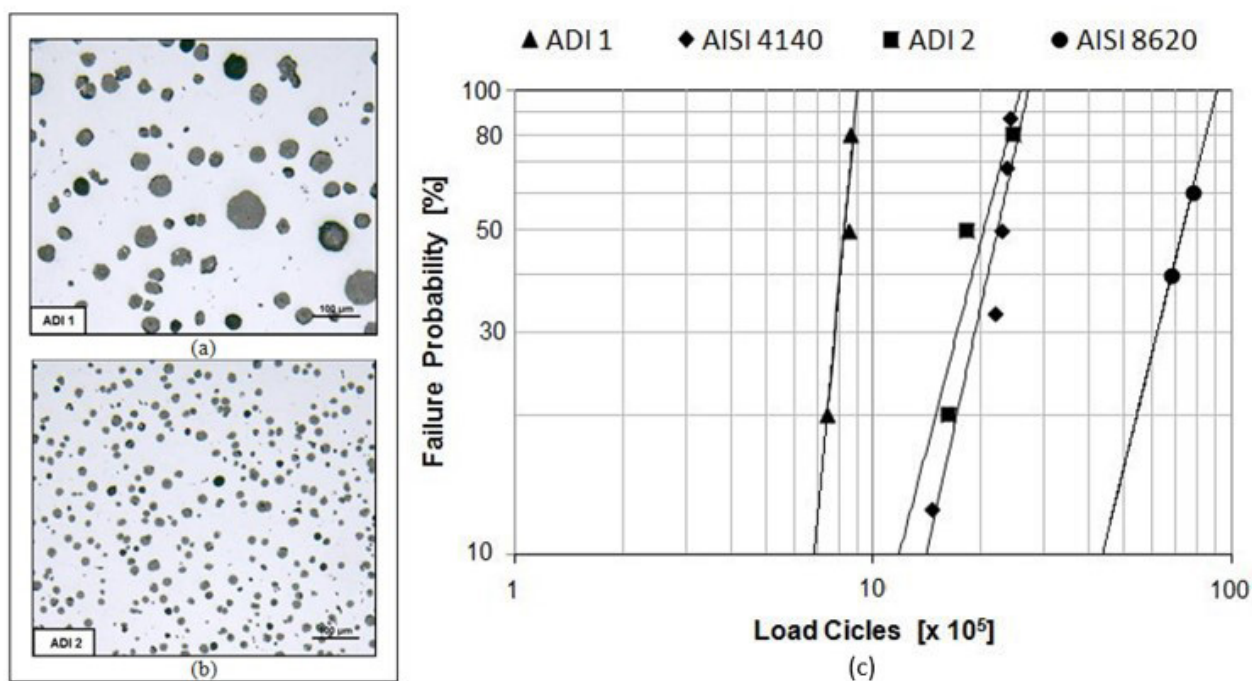


Figure 1. FZG test on ADI gear: (a) Image of ADI 1 nodules; (b) Image of ADI 2 nodules; and (c) Weibull curve for 4% of *pitting* damage on the face of teeth [11].

Table 1. Percent weight composition, heat and thermochemical treatment [11]

ADI 1	C	Mn	Si	Cr	Mo	Cu	Mg
	3.1	0.2	2.3	0.03	0.3	0.7	0.04
	Austenitization Temperature = 890 °C / Time = 2 hours						
	Austempering Temperature = 290 °C / Time = 2 hours (in salt bath)						
ADI 2	C	Mn	Si	Cr	Mo	Cu	Mg
	2.8	0.4	2.4	0.02	-	0.6	0.03
	Austenitization Temperature = 900 °C / Time = 2 hours						
	Austempering Temperature = 270 °C / Time = 2 hours (in salt bath)						

3 Results

The studies shown in Table 4 have brought extremely important results for the general understanding of the ADI behavior and explaining in part the experimental results obtained in Guesser et al. [11]. The results were divided according to the load type applied to the gear teeth, with the gear tooth root being subjected to bending stresses and the tooth face subjected to contact stresses.

Table 2. Gear type C parameters [13]

Parameter	Unit	Pinion	Wheel
Number of teeth - Z	-	16	24
Module - m	mm		4.5
Center distance	mm		91.5
Pressure angle - α	°		20
Face width - b	mm		14
Addendum modification - x	-	+ 0.182	+ 0.171

Table 3. ADI mechanical properties and nodules characteristics [11]

Characteristic	Unit	ADI 1	ADI 2
Ultimate tensile strength	MPa	1546	1273
Elongation	%	2.1	3.5
Young's modulus	GPa	183.9	186.9
Hardness	HRC	56	54
Average nodules diameter	μm	29.1	17.6
Nodularity	%	99	98
Percentage of graphite	%	13	13
Nodule density	nodules/ mm^2	196	532
Average distance between nodules	μm	80	36
Average distance/diameter ratio	(-)	2.75	2.05

- Graphite nodule: Young's modulus = 35 GPa and Poisson's ratio = 0.126 [14]; ADI matrix: Poisson's ratio = 0.25 [3].

3.1 Gear tooth root region – bending fatigue

One of the first decisions to be implemented in the numerical analysis was the option to use submodeling tools. This serves to refine the mesh in the region of interest and to be able to observe the microstructural effects of the nodules that have micrometric dimensions.

Bru [18], performing a 3D analysis, sought to understand how the size, number of nodules and their position in relation to the surface affect the state of stress in its neighbor. It was then observed what happened with the stress concentrating geometric factor (K_t) represented by the presence of the nodule when the tooth is submitted to bending. The results showed that the stress field generated by the nodules undergoes a homogeneous stress relief when we analyze nodules positioned parallel to the surface. Figure 3 shows an analysis of von Mises stresses in relation to the presence of nodules vertically on the surface. A reduction in tensions is perceived as it moves away from the surface, with an evident influence on K_t . In the other analyzes performed, it can be summarized that the presence of nodules induces concentration factors (K_t) between 1.4 and 1.65. These results were inferior to traditional analytical studies of bending K_t in drilled parts, as well as other numerical analysis (also with nodules) in two dimensions. These results show the importance of a more critical assessment of the comparison between 2D and 3D analysis.

Lazzaron [19] performed similar analyzes to Bru [18], but in a 2D environment. She identified a strong influence of the tooth root edge on the values of K_t arising from the presence of nodules, always presenting higher values. Further intensifying the surface as a great bending damage nucleator, especially for nodules up to 8 μm . The results with

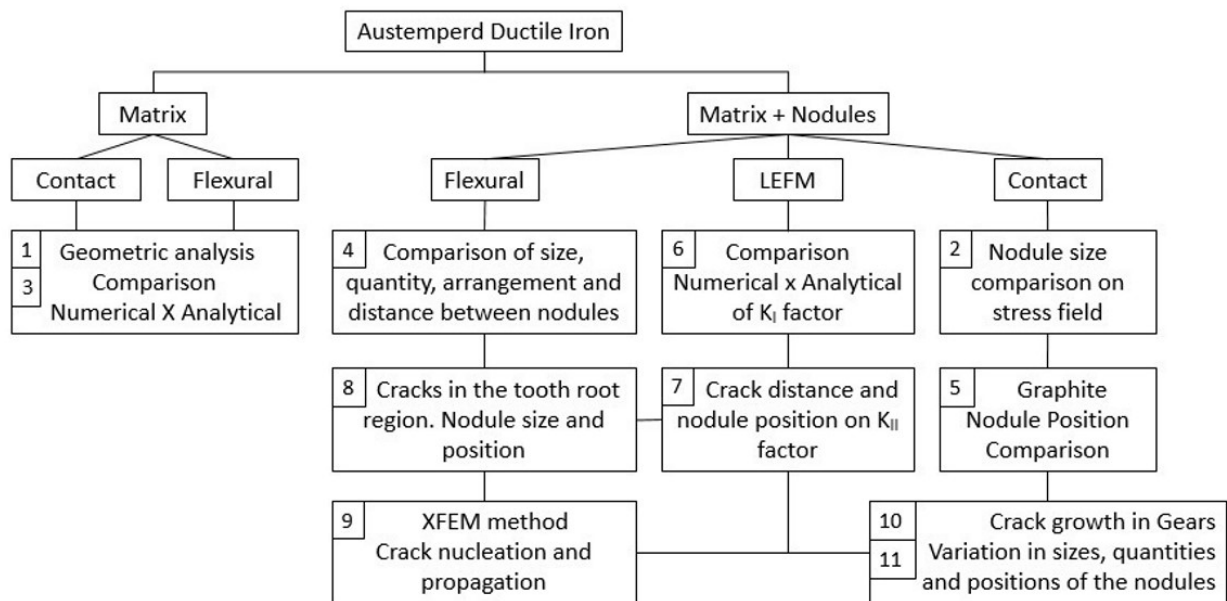


Figure 2. Flowchart of FEM studies covering ADI.

Table 4. Works performed with FEM

	Title	Details of FEM analysis	Goal	Author
1	Análise das tensões de contato em engrenagens utilizando os métodos analítico e numérico	<ul style="list-style-type: none"> · ANSYS Workbench · Mesh: 461468 nodes · 315686 elements · Three-dimensional analysis 	Compare numerical solutions by FEM with analytical solutions.	Reisdorfer and Gequelin [15]
2	Numerical Analysis of the Influence of Graphite Nodule Size on the Pitting Resistance of Austempered Ductile Iron Gears	<ul style="list-style-type: none"> · ANSYS Workbench · 189665 elements · Empty nodules representation · Three-dimensional analysis · 100% nodularity · Submodeling 	Analysis of isolated nodules and stress field contribution to stress concentration factors.	Gans et al. [16]
3	Analysis of the relation between the flexural stress and the geometrical variations in spur gears using modified Lewis? Equation and numerical methods	<ul style="list-style-type: none"> · ABAQUS · Several partitions in local focus · Hexagonal finite elements · Element size = 0.1 mm · Plane strain state · Submodelling 	Compare numerical solutions by FEM with analytical solutions for bending stresses.	Quadros et al. [17]
4	Uso do método de elementos finitos no estudo das tensões de flexão em engrenagens de ferro fundido nodular austemperado	<ul style="list-style-type: none"> · ABAQUS · Mesh from 4 mm to 0.05 mm · Three-dimensional analysis · Field history output · Submodelling · Plane strain state 	Effect of size and distance between nodules on tooth root propagation.	Bru [18]
5	Efeito do tamanho e distribuição de nódulos de grafita na propagação de trincas de fadiga de contato em ferros fundidos nodulares austemperados (ADI)	<ul style="list-style-type: none"> · ABAQUS · Element size from 1 to 0.1 mm · Submodeling · Refinement of “local seeds” mesh · Contour Integral Method · Crack propagation by Python 	Behavior of the nucleated crack in the tooth root region. Manual and automated way.	Lazzaron [19]
6	Influência das características dos nódulos no comportamento de trincas em matriz de ferro fundido	<ul style="list-style-type: none"> · ABAQUS · 2 to 4 mm pre-crack · Crack increment by re-meshing · Two-dimensional analysis · compact tension (CT) specimen of LEFM 	Comparison between numerical and analytical stress intensification factors K_I e K_{II}	Suginoshita et al. [20]
7	A Finite Element Study of the Influence of Graphite Nodule Characteristics on a Subsurface Crack in a Ductile Cast Iron Matrix under a Contact Load	<ul style="list-style-type: none"> · ABAQUS · Submodelling · Plane strain state · Two-dimensional standard global model 	Effect of crack distance and nodule position on stress intensity factor K_{II}	Suginoshita et al. [21]
8	A finite element study of the influence of graphite nodules size on subsurface contact stress of austempered ductile iron gear	<ul style="list-style-type: none"> · ANSYS Workbench · Global analysis and submodelling · Plane strain state · Mesh from 0.8 mm with “Sizing” command 	Effect of size and position of nodules in relation to regions of maximum contact stress.	Lazzaron et al. [22]
9	Numerical simulation for crack propagation in gear teeth using the extended finite element method	<ul style="list-style-type: none"> · ABAQUS / XFEM · Cohesive segments method · Phantom nodes · Maximum principal stress criterion for crack initiate · Fracture energy criterion for propagation 	Influence of the size and distribution of nodules on the propagation behavior of fatigue cracks.	Quadros et al. [23]

Table 4. Continued...

Title	Details of FEM analysis	Goal	Author
10 Estudo numérico bidimensional de propagação de trincas em ferro fundido nodular austemperado (ADI)	<ul style="list-style-type: none"> · ABAQUS · Python programming · Submodelling · Element CPE8R (8 nodes) · Plane strain state 	Modeling with multiple nodules and development of the $da/dN \times DK_{eff}$ curve.	França [24]
11 Bidimensional numerical study of crack propagation on austempered ductile iron	<ul style="list-style-type: none"> · ABAQUS · Python programming · Submodelling · Element CPE8R (8 nodes) · Plane strain state 	Comparison of the crack growth rate for materials ADI1 and ADI2.	França et al. [25]

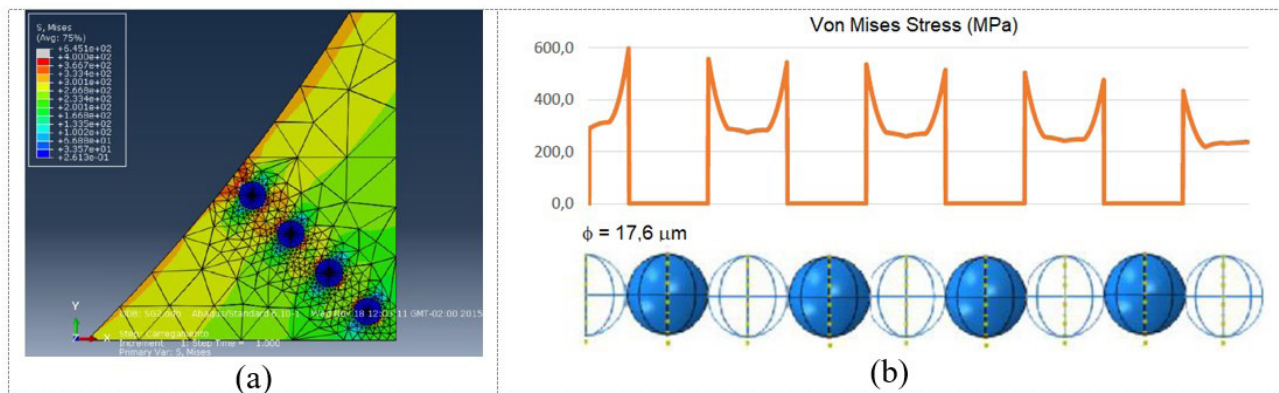


Figure 3. FEM-3D analysis: (a) Stress field image for graphite nodules arranged in the normal direction to the tooth root surface; (b) Von Mises stress variation, passing through the center of the nodule, from the surface of the tooth root towards the tooth core (distance from a nodule) [18].

nodules of 16, 32, 64 and 128 μm show that the values of Kt practically remain constant from a distance of 0.10 mm. Varying between 1.7 and 1.8, that is, for most cases, from this distance of 0.10 mm onwards, the nodule size is no longer relevant to the stress concentration.

In order to go a step further and incorporate concepts from LEFM, Lazzaron [19] also investigated the influence of graphite nodules (dispersed in the ausferritic matrix) on the crack behavior located in the tooth root. In other words, after the entire crack nucleation step, where the Kt factor was shown to be important as an agent for the onset of damage. It will now be studied how a crack submitted to bending stresses in the graphite nodules presence behaves. A strong influence on the stress intensity factor (in fracture mode I) K_I was observed in the nodules presence close to the crack tip. The drop in K_I is more intense for nodules positioned in front of the crack (0° alignment) than when they are positioned at 45° . The larger is the diameter of the nodule, the greater is the influence on the values of K_I . This influence being increasingly greater as the nodules are approached to the crack tip.

The crack tends to slant in the presence of nodules located outside its natural propagation path. The larger the nodule diameter, the greater the crack deviation angle (propagation), as can be seen in Figure 4. It is remarkable

the direction deviation in crack propagation, starting in iteration 5 and as well as in iterations 7 and 9 following it.

In the work by Quadros et al. [23], a damage evolution analysis tool, modeled with the Extended Finite Element Method (XFEM) within in the Abaqus software, was employed. Figure 5 shows one of the XFEM advantages with the possibility of cracks nucleating on the tooth surface (images (a) and (b)), with an intense effect of the nodules size in the crack propagation direction. And also with cracks nucleating, from the higher stress concentration at the matrix-nodule interface (images (c)) and the crack propagation occurring in both directions: to surface and to tooth bore.

Figure 6 shows a close-up analysis of a real microstructure with nodules of various sizes and randomly scattered in the material core (images (a) and (b)). In images (c) to (f) there is a greater effect on the crack tip stress field when it passes close to a larger diameter nodule and also the possibility of a crack crossing the nodule. With nucleation, almost diametrically opposite to the arrival position arrival of the crack to the nodule. This crack branching mechanisms cited by Greno et al. [26], works as a rate limiter of crack propagation. This phenomenon acts strongly in the tooth root region, but it can also be one of the factors that is related to the higher ADI 2 performance in relation to the ADI1 in the contact fatigue tests, which is the subject of the next section.

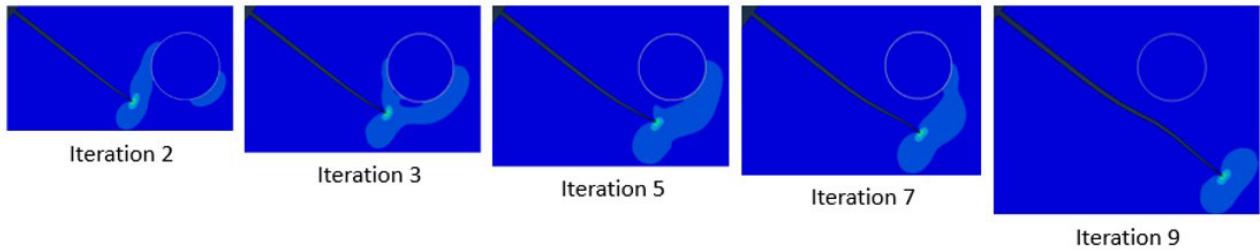


Figure 4. Crack propagation evolution influenced by the nodule presence [19].

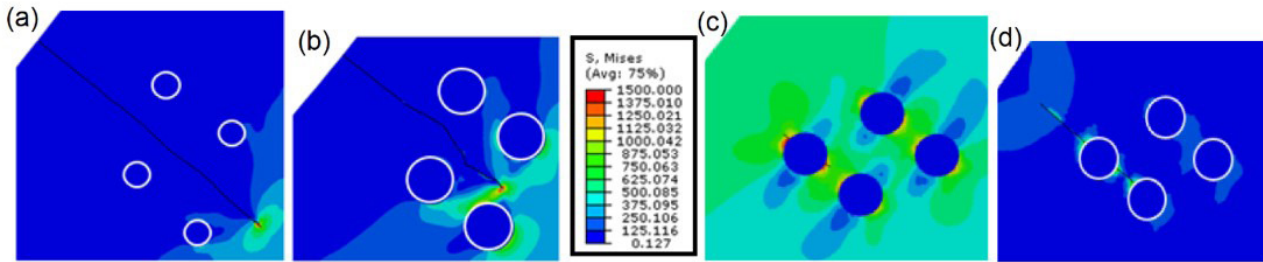


Figure 5. Surface nucleated crack propagation: (a) 16 μm nodule; (b) 32 μm nodule. 16 μm nodules: (c) crack nucleation in nodules; (d) crack propagation to surface and to bore [23].

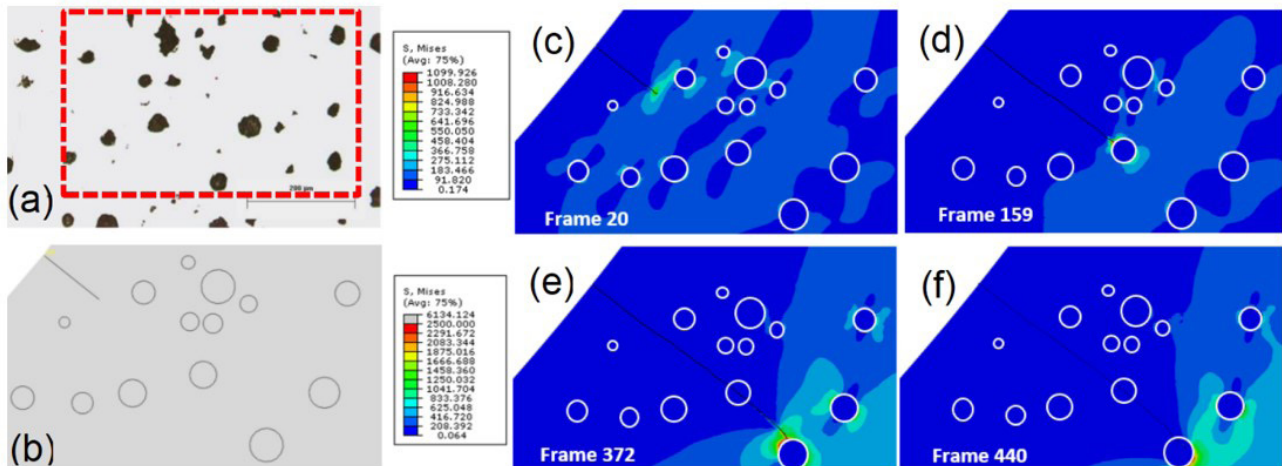


Figure 6. (a) ADI micrograph, (b) schematic drawing of the nodules positioning with different sizes, (c to f) frames 20, 159, 372 e 440 of crack propagation [23].

3.2 Gear tooth face region – contact fatigue

In order to understand the contact stresses state on the tooth faces in Type-C gears, Reisdorfer and Gequelin [15] compared the state of surface and sub-surface stresses calculated analytically according to Hertz [27] and numerically using FEM. Figure 7a shows an example of the stress distribution with the contact occurring in the HPSTC region (highest point single tooth contact) and Figure 7b a comparative table showing that the greatest difference in Von Mises maximum stress does not exceed 4.52%. Thus providing certainty as to the results of the numerical methodology developed.

The next step was to incorporate the presence of nodules in the ADI matrix and begin to understand the combined effect of nodule size and matrix stiffness. First, it was decided to consider the nodules as empty in the ausferritic matrix. Gans et al. [16] analyzed the stress fields for an isolated nodule (Figure 8a) positioned at a distance of 100 μm from the surface, obtaining numerical stress concentration factor (K_{ntms}) values around 2.40 and 2.45 for ADI 1 and ADI 2 respectively. In order to verify the influence of more nodules in the region where subsurface shear stresses are higher (Figure 8b), several nodules were positioned along the depth of the material (distanced by

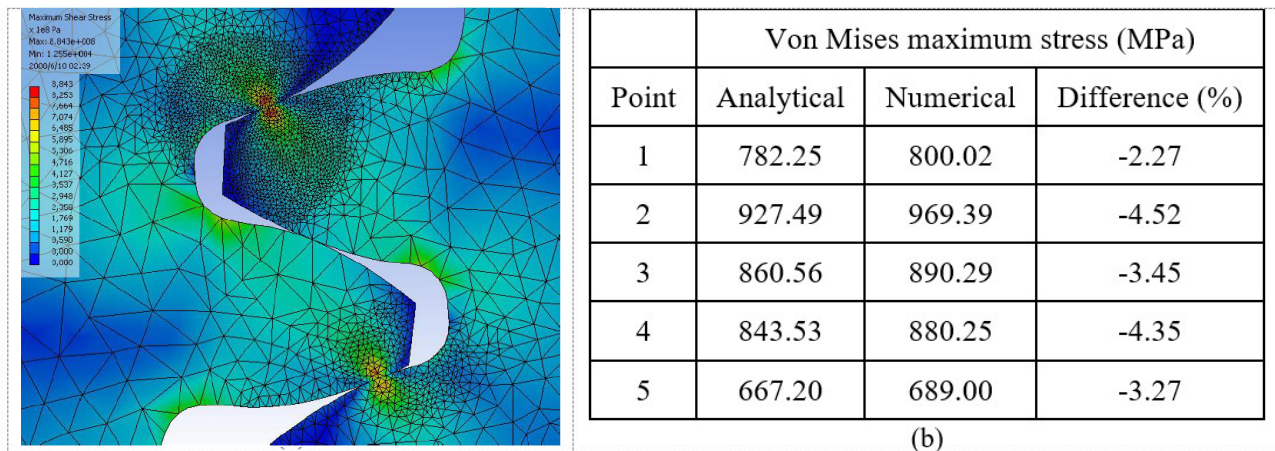


Figure 7. Results of FEM analysis of C-type gears without nodules: (a) Stress field distribution; (b) Comparative table between the analytical model of Hertz and the numerical analysis [15].

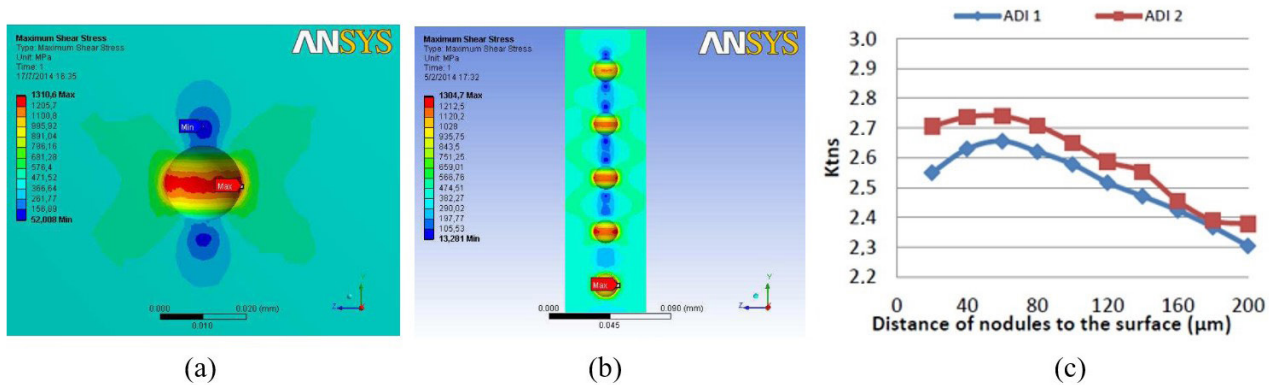


Figure 8. Nodule alone condition (a), multiple nodule strung condition (b) and shear stress concentration factor graph (c) [16].

20 μm). By comparing the factor of shear stress concentration (*K_{tns}*) due to the nodule presence (Figure 8c), it can be identified that: (i) the depth where the maximum shear stress, responsible for crack nucleation in contact fatigue, shifts from 100 to 60 μm; (ii) near the surface, the presence of smaller nodules (ADI2) causes higher tensions at the matrix-nodules interface, making it a material with greater crack nucleating potential and, consequently, with a lower number of fatigue cycles than ADI1.

In the simulations performed by Lazzaron et al. [22], with nodules positioned horizontally and vertically to the contact surface (Figure 9a), it is possible to observe that for only a nodule located at the depth of higher shear contact stresses, the shear stress concentrating factor (*K_{tns}*) does not change for larger nodule diameters (Figure 9b).

In Figure 10, it is possible to observe that when the positioning of the nodules is perpendicular to the flow lines, the influence of the second nodule is very small, not reaching values greater than 1% for any spacing between nodules. However, when the nodules are positioned parallel to the flow of the compressive forces, for distances between nodules in the range of 1 to 2 x diameter, there is a stress

relief behavior, reducing about 3.5% for ADI 1 and 4.4% for ADI 2.

When the LEFM approach is employed, understanding the interaction between the crack tip and the stress field developed by the presence of the graphite nodule is very important, because in the region of contact between gear teeth, efforts compressive combined with shears (rolling + sliding) change parameters such as propagation velocity and also crack propagation direction. Suguioshita et al. [20] observed that an increase in *K_I* occurs when the crack is close to a nodule. In situations where the nodule diameter is larger (Ex: ADI 1), the *K_I* values are higher in relation to smaller diameter nodules (ADI 2), especially for small distances. When comparing *K_I* values at the tip of a crack present in a ferritic matrix without nodules, with the same crack situation in the nodules presence, if the size of the nodules is similar to those of ADI 1 and ADI 2, *K_I* reaches values of 55.5% and 47.5% higher, respectively. Again, the propagation speed of a crack in an environment with large nodules is higher compared to smaller nodules.

The results of simulations performed by França [25], using the model represented in Figure 11a, showed that the

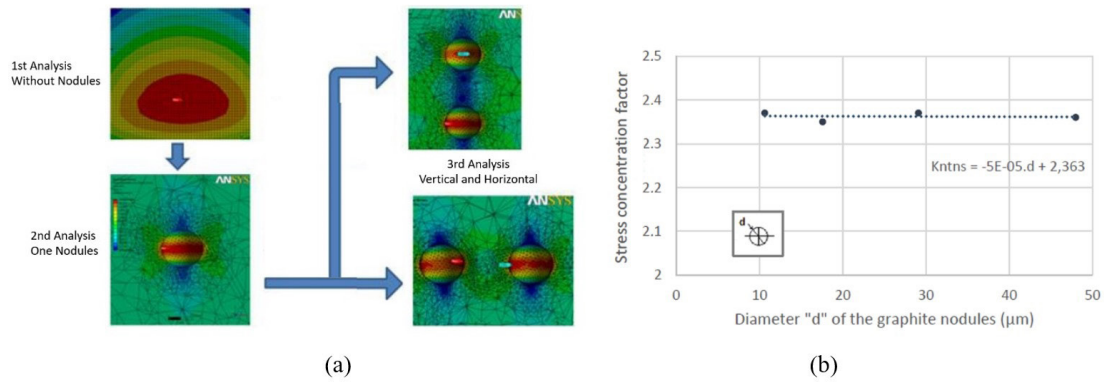


Figure 9. FEM analysis: (a) Sequence of study to observe the behavior of stress field; (b) Von Mises stress concentration factor for four different nodule size [22].

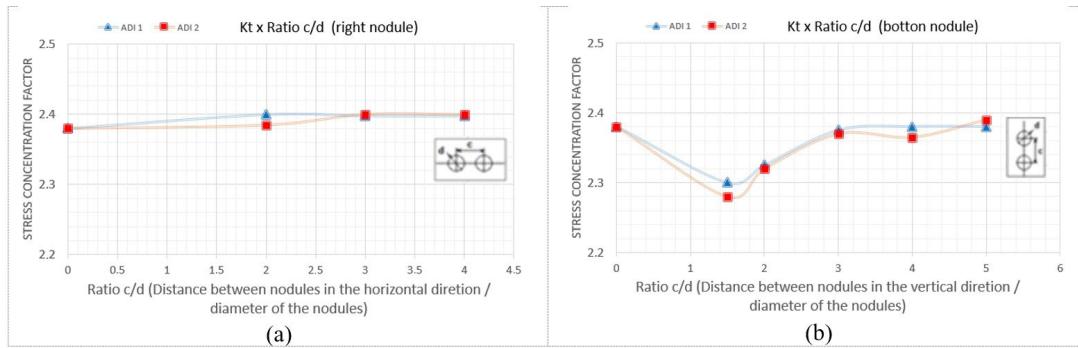


Figure 10. Graphs of K_t analysis: (a) nodules positioned horizontally (perpendicular to the flow lines) and (b) nodules positioned vertically (parallel to the flow lines) [22] modified.

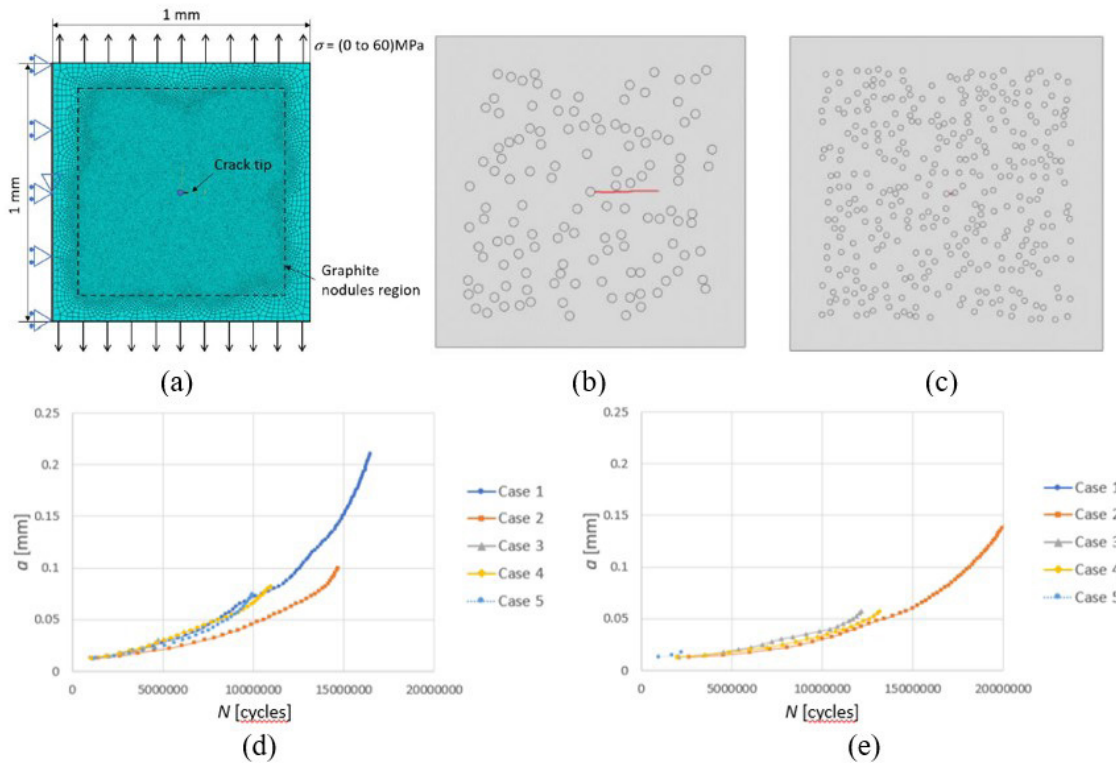


Figure 11. Geometry and boundary conditions (a), crack propagation for different amounts and sizes of nodules (b) and (c). Results of curves $a - N$ for ADI 1 (d) and ADI 2 (e) [25].

presence of a nodule generates a shear stress at the crack tip, which is the main parameter responsible for changing the crack direction. Modifications such as increasing the size of the nodule and decreasing the distance from the nodule to the tip of the crack intensify this action. In simulations with two ADI with different nodule diameter and with the same graphite area fraction, the increase in the number of nodules makes the crack have a shorter service life until it intercepts a new nodule. As can be seen in Figure 11c compared to Figure 11b and in the graphs of Figure 11d and Figure 11e. Therefore, this suggests that the protective effect of smaller nodules may be correlated with the number of intercepted nodules. Thus, the energy required to make a crack nucleate again and go back inside the matrix is much greater. This fact leads to lower propagation of pitting-forming cracks and, consequently, presenting greater resistance to this type of damage from contact fatigue.

4 Conclusion

The use of computational tools, such as the finite element method, to study the fatigue behavior of materials with such heterogeneous microstructure as ADI, is an extremely valuable form of analysis, which can become an aid tool in the phases of iron alloy design and/or material selection for an application with dynamic stresses.

Both in the studies of bending fatigue at the teeth root and in those of contact fatigue, it was possible to identify different behaviors with the implementation of changes in the size and distribution of graphite nodules in the matrix.

The combined analysis of parameters from traditional solids mechanics (stress concentrating factors - K_t) with those from linear elastic fracture mechanics (stress intensifier factor - K_I and K_{II} ; crack propagation angle - θ) proved capable of to support the understanding of the behavior of two types of ADI in contact fatigue test in FZG type test.

From the bending stresses point of view, the presence of nodules very close to the tooth root surface cause a higher possibility of crack nucleation. Even the maximum stresses occurring on the tooth surface, it is possible for cracks to appear, nucleated at the nodule-matrix interface, and propagation may follow the direction of the bulk of the

material to the surface, or the crack may grow towards the core of the gear tooth.

From the analyzes carried out in the contact region, it is possible to identify a series of results that help us to understand these materials behavior. The main results are: (i) the presence of nodules in the contact region causes the maximum shear stresses (generally determined by the Hertz equations) migrating closer to the surface; (ii) the analyzes carried out with several nodules show that the stress field altered by the nodules presence is affected by the size and proximity between the nodules and, in many situations, may have a beneficial effect of stress relief; (iii) in addition to the nodules, the elastic properties of the ferritic matrix contribute to fatigue crack propagation phase. Finally, nodules size and their distribution relationship are of paramount important because although ADI 2 has a small tendency in nucleating cracks faster than ADI 1, the greater number of nodules act as blocking elements to crack propagation, tending to form a network of cracks and reducing damage in pitting form.

Nomenclature

ADI – Austempered Ductile Iron
 FEM – Finite Element Method
 UTFPR – Universidade Tecnológica Federal do Paraná
 FZG – Forschungsstelle für Zahnräder und Getriebebau
 AISI – American Iron and Steel Institute
 C – Carbon
 Mn – Manganese
 Si – Silicon
 Cr – Chromium
 Mo – Molybdenum
 Cu – Copper
 Mg – Magnesium
 LEFM – Linear Elastic Fracture Mechanics
 K_t – Stress Concentrating Geometric Factor
 K_I – Stress Intensity Factor - mode I
 K_{II} – Stress Intensity Factor - mode II
 XFEM – Extended Finite Element Method
 K_{ntns} – Numerical Shear Stress Concentration Factor with nodules

References

- 1 Aranzabal J, Serramoglia G, Gorla CA, Rousière D. Development of a mixed (ferritic-ausferritic) ductile iron for automotive suspension parts. *International Journal of Cast Metals Research*. 2003;16(1-3):185-190.
- 2 Guesser WL, Guedes LC. Desenvolvimentos recentes em ferros fundidos aplicados à indústria automobilística. In: *Seminário da Associação de Engenharia Automotiva – AEA; 1997; São Paulo*. São Paulo: AEA; 1997 [cited 2021 Aug 20]. Available at: https://www.tupy.com.br/downloads/guesser/desenv_ferros_fund.pdf
- 3 Guesser WL. *Propriedades mecânicas dos ferros fundidos*. São Paulo: Blucher; 2009.
- 4 Blackmore PA, Harding RA. The effects of metallurgical process variables on the properties of austempered ductile irons. *Journal of Heat Treating*. 1984;3(4):310-325.

- 5 Guedes LC, Guesser WL, Duran PV, Santos SBA. Utilização de ferros fundidos nodulares bainíticos na fabricação de engrenagens. *Metalurgia ABM*. 1986;42:237.
- 6 Tun T, Twin KT. Optimizing the microstructure and mechanical properties of austempered ductile iron for automobile differential gear. *Journal of Metals, Materials and Minerals*. 2008;12:199-205.
- 7 Gorla C, Conrado E, Rosa F. Contact and bending fatigue behavior of austempered ductile iron gears. *Proceedings of the Institution of Mechanical Engineers, Part C*. 2017;232:998-1008.
- 8 Zammit A, Bonnici M, Mhaede M, Wan R, Wagner L. Shot peening of austempered ductile iron gears. *Surface Engineering*. 2017;33(9):679-686.
- 9 Concli F. Austempered Ductile Iron (ADI) for gears: Contact and bending fatigue behavior. *Procedia Structural Integrity*. 2018;8:14-23.
- 10 Pedro DI, Dommarco RC. Rolling contact fatigue resistance of Carbide Austempered Ductile Iron (CADI). *Wear*. 2019;418-419:94-101.
- 11 Guesser WL, Koda F, Martinez JAB, Da Silva CH. Austempered ductile iron for gears. Warrendale: SAE International; 2012. p. 1-10. (SAE Technical Paper; no. 36) [cited 2021 Aug 20]. Available at: <https://www.tupy.com.br/downloads/guesser/adi-engrenagens.pdf>
- 12 Martinez JA. Comparação da resistência ao desgaste por fadiga de contato de engrenagens fabricadas em aço AISI4140 e ferro fundido nodular austemperado [dissertation]. Curitiba: Universidade Tecnológica Federal do Paraná; 2011.
- 13 Koda F. Estudo da fadiga de contato em engrenagens cilíndricas de dentes retos [dissertation]. Curitiba: Universidade Tecnológica Federal do Paraná; 2009.
- 14 Yan W, Pun CL, Wua Z. Some issues on nanoindentation method to measure the elastic modulus of particles in composites. *Composites. Part B, Engineering*. 2011;42(8):2093-2097.
- 15 Reisdorfer DB, Gequelin J. Análise das tensões de Contato em Engrenagens utilizando os métodos analítico e numérico [trabalho de conclusão de curso]. Curitiba: Universidade Tecnológica Federal do Paraná; 2008.
- 16 Gans LHA, Guesser WL, Luersen MA, Silva CH. Numerical analysis of the influence of graphite nodule size on the pitting resistance of austempered ductile iron gears. *Advanced Materials Research*. 2015;1120-1121:763-772.
- 17 Quadros PMS, Betim VT, Ferreira APCS, Da Silva CH. Analysis of the relation between the flexural stress and geometrical variations in spur gears using modified Lewis' equation and numerical methods. *Revista Internacional de Pesquisa em Engenharia*. 2016 [cited 2021 Aug 20];2:16-35. Available at: <https://periodicos.unb.br/index.php/ripe/article/view/21797>
- 18 Bru LBW. Uso do método dos elementos finitos no estudo das tensões de flexão em engrenagens de ferro fundido [trabalho de conclusão de curso]. Curitiba: Universidade Tecnológica Federal do Paraná; 2015 [cited 2021 Aug 20]. Available at: http://repositorio.utfpr.edu.br/jspui/bitstream/1/10348/2/CT_DAMEC_2016_2_30.pdf
- 19 Lazzaron J. Análise numérica do crescimento de trinca sob influência de nódulos de grafita submetida à flexão presente na raiz de dentes de engrenagem [trabalho de conclusão de curso]. Curitiba: Universidade Tecnológica Federal do Paraná; 2016 [cited 2021 Aug 20]. Available at: http://repositorio.utfpr.edu.br/jspui/bitstream/1/10490/1/CT_DAMEC_2016_2s_12.pdf
- 20 Suguinoshita G, Luersen MA, Silva CH. Influência das características dos nódulos no comportamento de trincas em matriz de ferro fundido. In: *Anais do 70º Congresso Anual da ABM*; 2015; Rio de Janeiro. São Paulo: ABM; 2015. p. 426-435 [cited 2021 Aug 20]. Available at: <https://abmproceedings.com.br/ptbr/article/influencia-das-caracteristicas-dos-nodulos-no-comportamento-de-trincas-em-matriz-de-ferro-fundido>
- 21 Suguinoshita G, Da Silva CH, Luersen MA. A finite element study of the influence of graphite nodule characteristics on a subsurface crack in a ductile cast iron matrix under a contact load. *Computer Modeling in Engineering & Sciences*. 2018;117(1):59-71.
- 22 Lazzaron J, Luersen MA, Silva CH. A finite element study of the Influence of graphite nodules size on subsurface contact stresses of Austempered Ductile Iron gears. In: *Proceedings of the 24th ABCM International Congress of Mechanical Engineering; COBEM'17*; 2017; Curitiba, PR, Brazil. Rio de Janeiro: ABCM; 2017.
- 23 Quadros PMS, Ferreira APCS, Silva CH. Numerical simulation for crack propagation in gear teeth using the extended finite element method. In: *Proceedings of the 25th ABCM International Congress of Mechanical Engineering; COBEM'19*; 2019; Uberlândia, MG, Brazil. Rio de Janeiro: ABCM; 2019.

- 24 França GVZ. Efeito numérico bidimensional de propagação de trincas em ferro fundido nodular austemperado (ADI) [dissertação]. Curitiba: Universidade Tecnológica Federal do Paraná; 2020 [cited 2021 Aug 20]. Available at: http://repositorio.utfpr.edu.br/jspui/bitstream/1/4731/1/CT_PPGEM_M_Franca%2c_Gustavo_von_Zeska_de_2019.pdf
- 25 França GVZ, Luersen MA, Da Silva CH. Bidimensional numerical study of crack propagation on austempered ductile iron. In: Proceedings of the XLI Ibero-Latin-American Congress in Computational Methods in Engineering; 2020. Belo Horizonte: ABMEC; 2020.
- 26 Greno GL, Otegui JL, Boeri RE. Mechanisms of fatigue crack growth in ADI. *International Journal of Fatigue*. 1999;21(1):35-43.
- 27 Johnson KL. Contact mechanics. Cambridge: Cambridge University Press; 1987.

Received: 20 Aug. 2021

Accepted: 15 Jan. 2022